

See discussions, stats, and author profiles for this publication at: <https://www.researchgate.net/publication/51549620>

Energy and Lifetime of Temporary Anion States of Uracil by Stabilization Method

ARTICLE *in* THE JOURNAL OF PHYSICAL CHEMISTRY A · AUGUST 2011

Impact Factor: 2.69 · DOI: 10.1021/jp205986z · Source: PubMed

CITATIONS

12

READS

81

2 AUTHORS, INCLUDING:



Ki Wi Chen

Tunghai University

12 PUBLICATIONS 115 CITATIONS

SEE PROFILE

Energy and Lifetime of Temporary Anion States of Uracil by Stabilization Method

Hsiu-Yao Cheng* and Chi-Wei Chen

Department of Chemistry, Tunghai University, Taichung 40704, Taiwan, R.O.C.

ABSTRACT: To investigate the temporary anion states of uracil, density functional theory with asymptotically corrected potentials is adopted. The stabilized Koopmans' theorem and stabilized Koopmans-based approximation are used in conjunction with an analytic continuation procedure to calculate its resonance energies and lifetimes. Results indicate the presence of several low-lying π^* and σ^* temporary anion states of uracil. The characteristics of these resonance orbitals are also analyzed. By comparing them with the experimental values and theoretical calculations, it is believed that the stabilization approach can provide more information on the resonance states.



1. INTRODUCTION

Temporary or metastable anion states are essential in understanding the electron interactions of biological molecules. Biochemical mechanisms, the radiation damage of genetic materials, and excess electron transfer in DNA are some of the examples. For instance, the important work of Sanche and co-workers showed that DNA strands could break through the decay of temporary anion states formed by low energy electron attachment.¹ This observation has inspired many experimental and theoretical investigations on DNA and RNA nucleobases.^{2–16} Many gas-phase experiments have studied dissociative attachment and electron-impact excitation/ionization of the nucleobases. Electron transmission spectroscopy (ETS) can be used to characterize the temporary anion states.^{17,18} Burrow and co-workers carried out ETS measurements for uracil, halouracils, and DNA bases.^{7,9} Based on computed orbital energies and scaled energy shifts, they have also estimated π^* and σ^* orbital energies for the nucleobases.^{7–9} Simons and co-workers proposed a resonant capture mechanism for strand break using ab initio calculations on DNA fragments.³ For the scattering calculations, Gianturco and Lucchese suggested the presence of three π^* and two σ^* low energy resonances for uracil.¹¹ Tonzani and Greene reported low-energy elastic electron scattering cross sections, including π^* resonance energies and widths, for uracil and four DNA nucleobases.¹² McKoy and co-workers reported low-energy elastic electron scattering cross sections and π^* resonance energies for constituents of DNA and RNA via Schrödinger multi-channel method.¹³ They have indicated the possible presence of a low-energy σ^* resonance for uracil.^{13a} Based on R-matrix calculation, Dora et al. reported three π^* resonances below 5 eV for uracil.¹⁴ Recently, Gianturco et al. suggested four π^* resonances for uracil.¹⁵

Because the temporary anion state lies energetically above the ground state of the neutral molecule, its electron affinity (EA) is negative. The theoretical calculation of negative EAs that reproduce ETS values is a challenging problem. This is due to the fact that the temporary anion is unstable with respect to electron

detachment. The variational calculations are likely to collapse to the neutral molecule plus a free electron for temporary anion states. The EAs are commonly computed via Koopmans' theorem (KT)¹⁹ approximation using Hartree–Fock (HF) or Kohn–Sham (KS) orbital energies. They are associated with the negative of the unfilled molecular orbital energies. However, most density functional theory (DFT)²⁰ potentials will not yield asymptotic behavior properly.^{21,22} The errors for Koopmans' EAs in conventional DFT can be of several electron volts. To remedy, various asymptotic correction (AC) schemes have been devised. In the long-range correction (LRC) scheme, the coulomb operator is usually divided into short-range (SR) and long-range (LR) parts by using the standard error function.^{23–26} Alternatively, Tozer and co-workers have proposed a Koopmans-based (KB) approximation using AC based on the consideration of the integer discontinuity in the exact exchange-correlation potential.²⁷

For temporary anion states, the energy calculations using the KT/KB approximations are unreliable. This is because the unfilled orbitals are prone to collapse onto approximations of continuum functions called orthogonalized discretized continuum (ODC)^{28–30} solutions when large basis sets are used. To distinguish the temporary anion orbital solutions from the ODC solutions, the stabilization method proposed by Taylor and co-workers³¹ can be used. The vertical attachment energies (AEs) are associated with the energies of the “stabilized” temporary anion states of the neutral molecules.^{28–30,32} By combining the stabilization method and consideration of LRC, we have recently applied the stabilized Koopmans' theorem (S-KT) and stabilized Koopmans-based approximation (S-KB) in studying the temporary anion states of a series of molecules.³² Results have indicated that the stabilization calculations via DFT

Received: June 25, 2011

Revised: August 5, 2011

Published: August 05, 2011

with AC potential can yield improvements in predicting energies of temporary anion states over other approaches.

So far, the stability of the resonance energies for nucleobases has not been systematically examined by the S-KT/S-KB approaches. In addition, the identification of the σ^* resonances has remained uncertain.^{10,11,13a,14,15} The main reason is that the temporary anion states associated with empty σ^* orbitals usually have shorter lifetimes and broader resonances than those associated with π^* orbitals. The breadth of the structures usually makes it difficult to assign the resonance energy accurately.⁸ Hence, it is fitting for us to investigate the nucleobases via the S-KT/S-KB method. In this study, we will focus mainly on the temporary anion states of uracil molecule. Both the S-KT using LRC density functional and the S-KB using local functional will be adopted. Then, their energies and lifetimes will be calculated. Finally, the results will be compared with experimental values and scattering calculations.

2. COMPUTATIONAL METHOD

The EA in the KT approximation can be written as $EA^{KT} \approx -\varepsilon_{VMO}$, where ε_{VMO} denotes the virtual molecular orbital energy. The vertical attachment energy, that is, the negative of EA, can then be represented as $AE^{KT} \approx \varepsilon_{VMO}$. The virtual orbital energy associated with temporary anion state is also known as AE. The AE obtained from KT approach will be denoted as ε_{VMO} . When the alternative KB approximation is adopted, the asymptotic correction of the Koopmans value is roughly represented as $\varepsilon_{HOMO} + (E_{N-1} - E_N)$. Here, ε_{HOMO} is used to denote the highest-occupied molecular orbital energy determined from the DFT calculation using a local exchange-correlation functional on the neutral system. The E_N and E_{N-1} are the total electronic energies of the neutral and cation, respectively. By applying the correction term, AE in the KB approximation can be written as $AE^{KB} \approx \varepsilon_{VMO} + [\varepsilon_{HOMO} + (E_{N-1} - E_N)]$.

To distinguish the temporary anion state solutions from the virtual ODC ones, the stabilization method is employed. Four different Gaussian-type basis sets, designated as A, B, C, and D, are employed in our calculations. Our convention is as follows. The 6-31G(d)+ α (sp) basis set A is formed by augmenting the 6-31G(d) basis set with the diffuse sp function multiplied by a scale factor α (denoted as $\alpha(sp)$) on the C, N, and O atoms. The sp functions have the exponents of 0.05624, 0.07068, and 0.09000 for the C, N, and O atoms, respectively. The basis set B is the 6-31++G(d,p) basis set with scaling of the exponents of diffuse "+" functions on the C, N, O, and H atoms. The basis set C is formed by the Dunning's DZP+ basis set³³ that is augmented with the diffuse s functions on the C, N, and O atoms. The exponents of augmented s functions are chosen to be the same as those of diffuse + functions. Then the outermost diffuse sp functions of C, N, and O atoms and the outermost s function on H are simultaneously scaled. The basis set D is the aug-cc-pvdz basis set³⁴ with scaling of the outermost diffuse s and p functions on the C, N, and O atoms and the outermost s function on the H atom. The inclusion of additional diffuse d or f polarization functions on C, N, and O is found to be of minor importance. The reason is that the changes in resonance energy are rather small (<0.1 eV).

The stabilization graphs are obtained by plotting the calculated energies (ε_{VMO}) as a function of the scale factor α . As α increases, one or more ODC solutions may approach the temporary anion orbital solutions in energy and can lead to avoided

crossings between the two types of solutions. In the study of resonance energies for all DFT calculations, the simplest "midpoint method" in Burrow et al. will be used first.²⁹ The energy of the temporary anion state is taken as the mean value of two eigenvalues involved in the avoided crossing, if it exists, at the α_{ac} of closest approach.³⁵ Then, the analytic continuation method will be adopted to estimate both resonance energies and lifetimes from the avoided crossings between the eigenvalues of the stabilization graphs.^{36,37} In the present study, the analytic continuation procedure is accomplished by means of (n,n,n) generalized Padé approximation (GPA)³⁶ in which the energy is represented by the following quadratic equation:

$$E^2 P + EQ + R = 0 \quad (1)$$

where P, Q, and R are the following nth-order polynomials in α

$$P(\alpha) = 1 + p_1\alpha + p_2\alpha^2 + \dots + p_n\alpha^n \quad (2)$$

$$Q(\alpha) = q_0 + q_1\alpha + q_2\alpha^2 + \dots + q_n\alpha^n \quad (3)$$

$$R(\alpha) = r_0 + r_1\alpha + r_2\alpha^2 + \dots + r_n\alpha^n \quad (4)$$

From $3n + 2$ pairs of data points $\{E_i, \alpha_i\}$, one can determine $3n + 2$ coefficients in eqs 2–4 by standard matrix method. Because GPA works best when data in the vicinity of avoided crossings are chosen, we always center the α range near α_{ac} to extract the resonance parameters. To determine a (3,3,3) GPA for $\alpha_{ac} > 0.4$, 10 points from both roots at $\alpha_i = \alpha_{ac}$, $\alpha_{ac} \pm 0.1$, $\alpha_{ac} \pm 0.2$, $\alpha_{ac} - 0.3$, and one point at $\alpha_i = \alpha_{ac} + 0.3$ from the lower root are used. As for $\alpha_{ac} < 0.4$, 10 points from both roots at $\alpha_i = 0.1, 0.2, \dots, 0.5$, and one point at $\alpha_i = 0.6$ from the lower root were used. To determine a (4,4,4) GPA for $\alpha_{ac} > 0.4$, 14 points from both roots at $\alpha_i = \alpha_{ac}$, $\alpha_{ac} \pm 0.1$, $\alpha_{ac} \pm 0.2$, $\alpha_{ac} \pm 0.3$ are used. As for $\alpha_{ac} < 0.4$, 14 points from both roots at $\alpha_i = 0.1, 0.2, \dots, 0.7$ are used. To determine a (5,5,5) GPA for $\alpha_{ac} > 0.5$, 16 points from both roots at $\alpha_i = \alpha_{ac}$, $\alpha_{ac} \pm 0.1$, $\alpha_{ac} \pm 0.2$, $\alpha_{ac} \pm 0.3$, $\alpha_{ac} - 0.4$, and one point at $\alpha_i = \alpha_{ac} + 0.4$ from the lower root are used. As for $\alpha_{ac} < 0.5$, 16 points from both roots at $\alpha_i = 0.1, 0.2, \dots, 0.8$, and one point at $\alpha_i = 0.9$ from the lower root are used. The stationary points, denoted as α^* , are obtained by solving $dE/d\alpha = 0$. The resulting α^* s are then substituted into the appropriate energy expression to obtain the corresponding complex stationary energies E^* s. The resonance state can be associated with $E^* = E_r - i\Gamma/2$, where E_r is the resonance position and Γ is the resonance width. The width is related to the lifetime τ via $\tau = \hbar/\Gamma$. Notice that, in addition to the physical stationary points, the analytic continuation procedure will give several spurious solutions. The spurious solutions tend to depend quite sensitively on the number and choice of input points used in the analytic continuation procedure. They can be distinguished from the physical solutions. The success of analytic continuation for locating complex stationary points depends on having input data of sufficient accuracy. In this study, the GPA calculations are performed in double precision. The input data E_i that come along with the kinetic energies of full MO results have six significant figures of accuracy. The sufficiently tight (10^{-9}) convergence criterion is used for the self-consistent field calculations.

In the present study, we adopt both (1) LRC functional via S-KT and (2) local functional via S-KB methods for the temporary anion states. For LRC functional, we use ω B97XD, LC- ω PBE, CAM-B3LYP, and LC-M06L functionals. The ω B97XD²³ functional includes LR HF exchange, a small fraction of SR HF exchange, a modified B97 SR exchange, B97 correlation

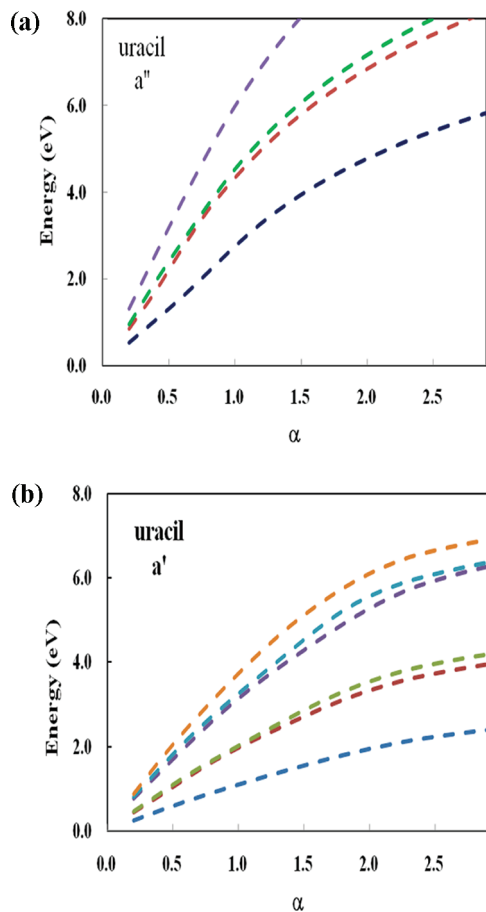


Figure 1. Energies of (a) a'' and (b) a' virtual orbitals as a function of α for a free electron in the absence of potentials using basis set A.

density functional, and empirical dispersion corrections. The LC- ω PBE²⁴ functional contains SR ω PBE exchange, LR HF exchange, and full range PBE correlation. The CAM-B3LYP²⁵ functional is comprised of 0.19 HF plus 0.81 Becke 1988 (B88) exchange interaction at SR, and 0.65 HF plus 0.35 B88 at LR. The LC-M06L functional applies the long correction of Hirao and co-workers²⁶ to the M06L³⁸ pure functional. The local functional chosen is the PBEPBE³⁹ pure generalized gradient approximation (GGA). In addition, (a) the hybrid M06 functional,⁴⁰ and hybrid meta GGA functionals of M06-HF⁴¹ and M06-2X,⁴⁰ (b) the double-hybrid functionals B2PLYP-D and mPW2PLYP-D that contain second-order perturbation corrections with long-range dispersion terms,⁴² and (c) the HF method will also be studied. All calculations are performed using the Gaussian 09 program⁴³ with geometric optimization of uracil being carried out at the B3LYP/6-31+G(d) level under C_s symmetry constraints.

3. RESULTS AND DISCUSSION

For the temporary anion shape resonance of uracil, we perform S-KT calculations for the ω B97XD, LC- ω PBE, CAM-B3LYP, LC-M06L, M06-HF, M06-2X, B2PLYP-D, mPW2PLYP-D, and HF (denoted as S-KT ^{ω B97XD}, S-KT^{LC- ω PBE}, S-KT^{CAM-B3LYP}, S-KT^{LC-M06L}, S-KT^{M06-HF}, S-KT^{M06-2X}, S-KT^{B2PLYP-D}, S-KT^{mPW2PLYP-D}, and S-KT^{HF}, respectively), and the S-KB calculations via PBEPBE, M06L, and M06 (denoted as S-KB^{PBEPBE}, S-KB^{M06L}, and

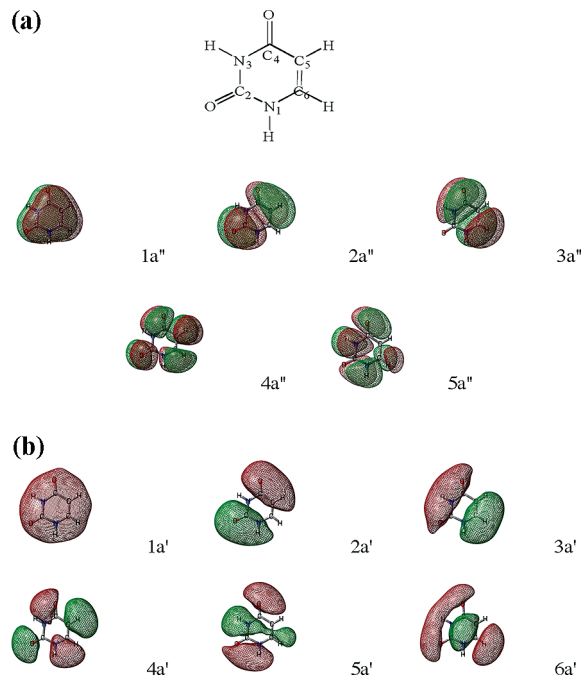


Figure 2. Plots of the (a) first five a'' virtual orbitals at $\alpha = 2.0$ and (b) first six a' virtual orbitals at $\alpha = 2.8$ for a free electron in the absence of potentials. The isosurface values are chosen to be 0.02 for all the orbital plots.

S-KB^{M06}, respectively) methods on the unfilled orbitals to distinguish them from the ODC solutions.

To distinguish the resonance and the ODC solutions of the molecular system, it is useful to study one-electron discretized continuum (1e-DC) solutions for a free electron. The energies of the 1e-DC solutions are obtained by solving a one-electron Schrödinger equation as described by the molecular basis set in the absence of any potential.²⁸ Figure 1a,b shows the energies of the 1e-DC solutions as a function of scale factor α using basis set A for the a'' and a' virtual orbitals of uracil located at appropriate nuclear positions, respectively. As shown in Figure 1, all 1e-DC solutions increase with α . We then examine the characteristics of 1e-DC solutions. Figure 2a,b shows the first five a'' 1e-DC solutions for $\alpha = 2.0$ and first six a' 1e-DC solutions for $\alpha = 2.8$. As can be seen from Figure 2, the numbers of nodal planes are 0, 1, 1, 2, and 2 for the first six a' virtual orbitals, respectively. In addition to the nodal plane of the ring, the first five a'' virtual orbitals have 0, 1, 1, 2, and 2 nodal planes azimuthally, respectively. Comparison of the energies and characteristics of the 1e-DC solutions with those of virtual orbitals from DFT/HF calculations on the actual molecule may allow one to determine which virtual orbitals correspond to temporary anion states.

In the C_s point group, the uracil molecule has 24 a' and 5 a'' occupied orbitals. The π/π^* orbitals are of A'' symmetry and the σ/σ^* orbitals are of A' symmetry. The stabilization graphs of the energies as a function of α using basis set A for the a'' and a' virtual orbitals of uracil for the S-KT ^{ω B97XD} calculations are shown in Figure 3a and b, respectively. There are two types of energies for virtual orbital solutions in the stabilization calculations. One is the unfilled orbital solution and the other is the ODC virtual orbital solution. The unfilled orbital solution and the ODC solutions are readily distinguished by examining how

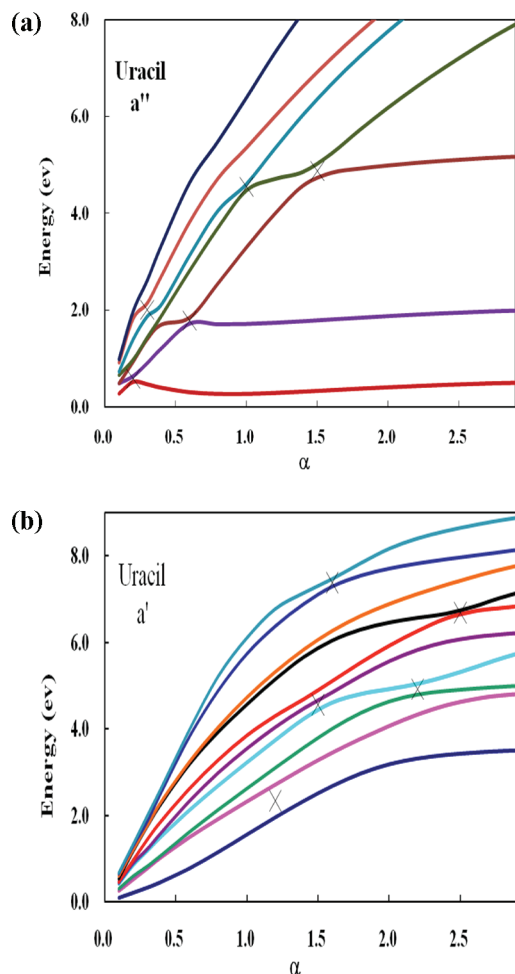


Figure 3. Stabilization graphs for uracil via S-KT ω B97XD method. Energies of (a) a'' and (b) a' virtual orbitals as a function of α using basis set A. The locations of α_{ac} are marked with x.

their energies vary with α and by comparing their solutions with the aforementioned 1e-DC solutions. First, we will present the results for the a'' virtual orbitals. By examining the nature of virtual orbitals of uracil as shown in Figure 2a, the first solution for $\alpha > 0.2$ that remains almost constant is mainly from the $6a''(\pi_1^*)$ orbital solution. The second solution for $\alpha > 0.6$ and the third one for $\alpha > 1.4$ are mainly from the $7a''(\pi_2^*)$ and $8a''(\pi_3^*)$ orbital solutions, respectively. The second solution for $0.2 < \alpha < 0.6$, third for $0.6 < \alpha < 1.4$, and fourth for $\alpha > 1.4$ that increase with α correspond to the first ODC solution. The fourth solution for $0.4 < \alpha < 1.0$ and fifth for $\alpha > 1.0$ are mainly from the second ODC solution. The avoided crossing resulted from the coupling between the first and second solutions is located at $\alpha_{ac}(1,2) = 0.2$. The energy of π_1^* orbital obtained is 0.57 eV at $\alpha_{ac}(1,2)$. The energies of π_2^* orbital obtained from the two avoided crossings are 1.79 eV at $\alpha_{ac}(2,3) = 0.6$ and 2.01 eV at $\alpha_{ac}(5,6) = 0.3$, respectively. The average value from each set of energy values will be defined as the energy of π_2^* orbital. Thus, the energy of the $7a''(\pi_2^*)$ orbital is 1.90 eV. The energies of π_3^* orbitals obtained from the two avoided crossings are 4.54 at $\alpha_{ac}(4,5) = 1.0$, and 4.88 eV at $\alpha_{ac}(3,4) = 1.5$, respectively. Hence, the energy of the $8a''(\pi_3^*)$ orbital is 4.71 eV. According to our observation, the avoided crossing at $\alpha_{ac}(1,2)$ is due to the coupling between π_1^* orbital and the first ODC solution.

Similarly, $\alpha_{ac}(2,3)$ is due to the coupling between π_2^* and the first ODC solution, the $\alpha_{ac}(5,6)$ between π_2^* and the fourth ODC solution, the $\alpha_{ac}(3,4)$ between π_3^* and the first ODC solution, and the $\alpha_{ac}(4,5)$ between π_3^* and the second ODC solution. Figure 4a displays the first seven a'' orbitals of uracil for $\alpha = 2.0$. As indicated in this figure, the first a'' virtual orbital, the LUMO, is from the π_1^* orbital. The second and third a'' orbitals are from the π_2^* and π_3^* orbitals, respectively. While the fourth, fifth, sixth, and seventh a'' orbitals containing extra diffuse function character are from the first, second, third, and fourth ODC solutions, respectively. As can be seen from Figure 4a, in addition to the nodal plane of the ring, the π_1^* , π_2^* , and π_3^* solutions have 2, 2, and 3 nodal planes azimuthally, respectively. As for the first four ODC solutions, they have 0, 1, 1, and 2 nodal planes azimuthally in addition to three nodal planes parallel to/containing the plane of the ring, respectively. The diffuse characteristics of the first four ODC solutions are similar to those of the first four 1e-DC solutions, as shown in Figures 2a and 4a.

Next for the a' σ^* virtual orbitals, the energy of the $25a'$ obtained from the avoided crossing is 2.34 eV at $\alpha_{ac}(1,2) = 1.2$. The energy of the $26a'$ obtained from the avoided crossing is 4.55 eV at $\alpha_{ac}(4,5) = 1.5$. The energy of the $27a'$ obtained from the avoided crossing is 4.92 eV at $\alpha_{ac}(3,4) = 2.2$. The energy of the $28a'$ obtained from the avoided crossing is 6.21 eV at $\alpha_{ac}(4,5) = 3.3$. The energies of the $29a'$ obtained from the avoided crossing are 6.69 eV at $\alpha_{ac}(6,7) = 2.5$ and 7.14 eV at $\alpha_{ac}(5,6) = 4.6$. The energies of the $30a'$ obtained from the avoided crossing are 7.39 eV at $\alpha_{ac}(9,10) = 1.6$ and 8.60 eV at $\alpha_{ac}(8,9) = 4.1$. Accordingly, the energies of the $29a'$ and $30a'$ orbitals are 6.91 and 7.99 eV, respectively. The resonance energies of π^* and σ^* orbitals can also be estimated from the stabilized energy values for $\alpha < 3.0$. They are very close to those obtained from the midpoint method except for $25a'$ orbital. The possible reason for the very broad $25a'$ resonance is that the basis may not be diffuse enough for α greater than about 2.2. In Figure 3b for $\alpha < 3.0$, the first solution for $\alpha > 1.2$ is mainly from the $25a'$ orbital solution. The fourth solution for $1.5 < \alpha < 2.2$ and the second one for $\alpha > 2.2$ are mainly from the $26a'$ orbital solution. The third solution for $\alpha > 2.2$ is mainly from the $27a'$ orbital solution. The fifth and sixth solutions for $\alpha > 2.5$ is mainly from the $28a'$ and $29a'$ orbital solutions, respectively. The ninth solution for $\alpha > 1.6$ is mainly from the $30a'$ orbital solution. The first solution for $\alpha < 1.2$, second for $1.2 < \alpha < 2.0$, and fourth for $\alpha > 2.2$ are mainly from the first ODC solution. For $\alpha > 2.5$, the seventh and eighth solutions correspond to the second and third ODC solutions, respectively. Figure 4b displays the first nine a' virtual orbitals of uracil for $\alpha = 2.8$. Based on the analysis of the nature of virtual orbitals, the first three a' virtual orbitals are mainly from the $25a'(\sigma_1^*)$, $26a'(\sigma_2^*)$, and $27a'(\sigma_3^*)$ orbitals, the fifth and sixth a' virtual orbitals are mainly from the $28a'(\sigma_4^*)$ and $29a'(\sigma_5^*)$ orbitals, and the ninth a' virtual orbital is mainly from the $30a'(\sigma_6^*)$ orbital, respectively. While the fourth a' virtual orbital containing extra diffuse s function character is mainly from the first ODC solution. The seventh and eighth a' virtual orbitals are mainly from the second and third ODC solutions. We then examine the bonding characteristics of σ^* MOs for uracil. As can be seen in Figure 4b, the $25a'$ orbital corresponds to strong antibonding between N₁-H, and between C₆-H, and bonding between N₁ and C₆, as well as between the H atoms attached to them. The $26a'$ orbital is primarily antibonding between N₃-H and between C₆-H. The $27a'$ orbital is mainly derived from

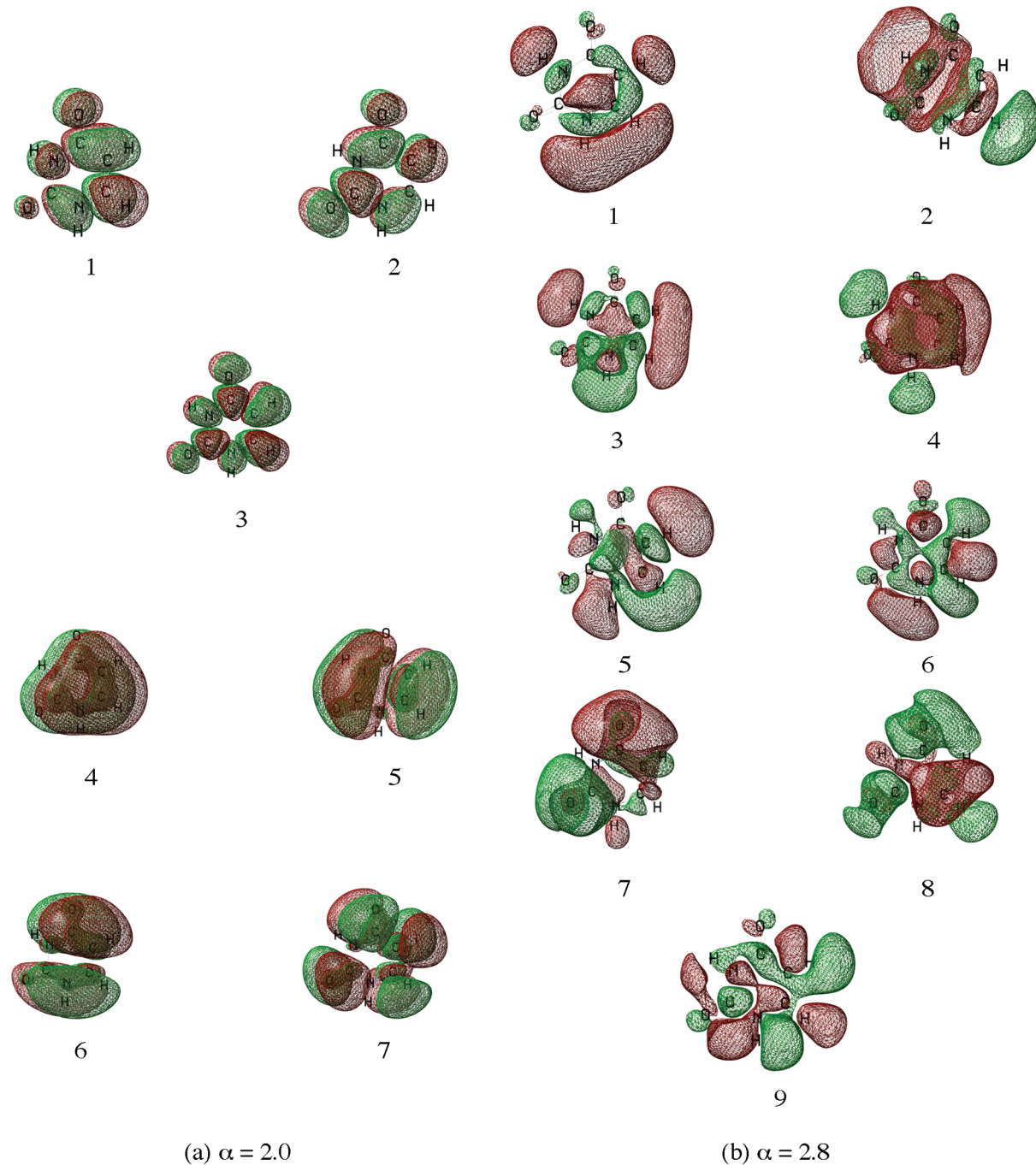


Figure 4. Plots of the (a) first seven a'' virtual orbitals at $\alpha = 2.0$ and (b) first nine a' virtual orbitals at $\alpha = 2.8$ for uracil. The isosurface values are chosen to be 0.02 for all the MO plots.

antibonding between N_1-H , between C_5-H , between C_6-H , and between N_1-C_6 . This orbital also has bonding between C_5 and C_6 , as well as bonding between the H atoms attached to them. The $28a'$ orbital is essentially from antibonding interaction between C_5 and C_6 , as well as antibonding between the H atoms attached to them. The $29a'$ orbital is mainly from antibonding between N_1-H , and bonding between C_5-C_6 . The $30a'$ orbital is essentially from antibonding between C_5-C_6 and a' of $N_1(2p)$. The three ODC solutions (the fourth, seventh, and eighth virtual orbitals) in Figure 4b have similar diffuse characteristics with those of the first three 1e-DC solutions in Figure 2b.

The calculated AEs of uracil using basis set A are tabulated along with the experimental values in Table 1. To compare with experimental results, corrected AEs are also included in the table. The corrected values are obtained by shifting the amount from the calculated AE values to bring the LUMO of uracil into agreement with the experimental values of Burrow et al.⁷ From the table, it can be seen that the AEs obtained from the S-KT^{HF} method are larger than those obtained from all of the DFT methods. The AEs obtained via the S-KT^{LC- ω PBE} and S-KT^{LC-M06L} methods are larger than those obtained from the other DFT methods. The AEs obtained from the S-KT^{M06-2X} method are

Table 3. Resonance Energies (E_r) and Widths (Γ ; eV) for Uracil Using Basis Set D

method	GPA	A''(π^*)					A'(σ^*)				
		E_r	0.36	1.69	4.58	2.35	4.35	4.82	6.07	6.75	7.57
present study (S-KT ^{wB97XD})	(3,3,3)	Γ	0.04	0.17	0.27	1.94	0.77	0.68	0.22	0.44	0.36
	(4,4,4)	E_r	0.36	1.74	4.56	2.31	4.31	4.77	6.04	6.64	7.42
		Γ	0.04	0.11	0.20	1.80	0.82	0.76	0.23	0.34	0.39
	(5,5,5)	E_r	0.36	1.75	4.52	2.20	4.28	4.68	5.99	6.63	7.50
		Γ	0.05	0.10	0.23	1.62	0.86	0.67	0.26	0.35	0.42
	(3,3,3)	E_r	0.08	1.51	4.33	1.68	3.87	4.11	5.16	6.45	7.42
		Γ	0.10	0.19	0.33	1.44	0.70	0.53	0.19	0.24	0.23
	(4,4,4)	E_r	0.08	1.50	4.33	1.53	3.78	4.10	5.08	6.37	7.45
		Γ	0.10	0.15	0.32	1.78	0.80	0.45	0.24	0.25	0.20
	(5,5,5)	E_r	0.06	1.52	4.27	1.52	3.86	4.18	5.05	6.46	7.49
		Γ	0.08	0.15	0.36	1.53	0.81	0.57	0.36	0.22	0.23
present study (S-KT ^{M06-HF})	(3,3,3)	E_r	0.44	2.04	5.29	1.96	4.32	4.50	5.55	6.88	7.46
		Γ	0.08	0.20	0.27	1.61	0.84	0.64	0.39	0.22	0.18
	(4,4,4)	E_r	0.46	2.05	5.32	1.96	4.22	4.47	5.49	6.74	7.41
		Γ	0.09	0.23	0.32	1.72	0.96	0.88	0.30	0.32	0.21
	(5,5,5)	E_r	0.46	2.06	5.40	1.84	4.15	4.49	5.55	6.71	7.39
		Γ	0.08	0.24	0.42	1.90	0.89	0.79	0.29	0.27	0.20
Burrow et al. ^a		E_r	0.216	1.609	5.009	2.26	3.67	3.87			
Winstead and McKoy ^b		E_r	0.32	1.91	5.08	1.45	4.5	4.5	6	6	8.5
Dora et al. ^c		Γ	0.018	0.16	0.40				6.17	7.62	8.12
Tonzani and Greene ^d		E_r	0.134	1.94	4.95				0.15	0.11	0.14
		Γ	0.003	0.168	0.38						
Leble et al. ^e		E_r	2.16	5.16	7.8						
		Γ	0.2	0.6	0.9						
Gianturco and Lucchese ^f		E_r	1.9	5.6	6.1	1.2	2.2		6.7		
		Γ	4.4			1.1	0.3		1.5		
Gianturco et al. ^g		E_r	2.27	3.51	6.50	0.012				10.37	
		Γ	0.21	0.38	1.03	0.46				0.84	
		E_r	0.33	1.70	3.50	6.50					8.29–8.47

^aThe resonance energies for a'' and a' orbitals are taken from the scaled virtual orbital energies of refs 7 and 8 respectively. ^bRef 13a. ^cRef 14. ^dRef 12. ^eRef 16. ^fRef 11. ^gRef 15.

0.27 eV, respectively. Thus, the resonance energy and width obtained for π_3^* orbital are 4.68 and 0.28 eV, respectively. Notice that all of the analytic continuation has been done assuming only two root crossings, but there are crossings as shown in Figure 3b that three roots could possibly be involved. However, the inclusion of the data points from the third root does not affect the results much. For instance, for 27a' orbital in Figure 3b, the (4,4,4) approximant employs energy data from the third and fourth curves at $\alpha = 1.9, 2.0, 2.1, 2.2, 2.3, 2.4$, and 2.5. The resonance energy and width yielded are 4.94 and 0.42 eV, respectively. When the input points at $\alpha = 2.0, 2.1, 2.2, 2.3, 2.4$, and 2.5 from the third curve, $\alpha = 1.9, 2.0, 2.1, 2.2, 2.3, 2.4$, and 2.5 from the fourth curve, and $\alpha = 1.8$ from the fifth curve are employed, the resonance energy and width yielded are 4.93 and 0.45 eV, respectively.

Table 3 tabulates the calculated resonance energies and widths using basis set D for the representative S-KT^{wB97XD}, S-KT^{B2PLYP-D}, and S-KT^{M06-HF} methods along with those of previous studies.^{7,8,11–16} As can be seen from the results, for the three π^* resonance energies, our calculations are in agreement with those of the previous studies by Burrow et al.,^{7,8} Winstead and McKoy,^{13a} and Dora et al.¹⁴ Previous scattering calculations by Tonzani and Greene, Leble et al., and

Gianturco and Lucchese yielded larger π^* resonance energies (1–2 eV) than ours. The more recent calculations by Gianturco et al. reported four π^* resonances. However, the 0.33 eV peak identified by Gianturco et al. as the π_1^* resonance appears to be computational artifact because the eight 2p orbitals of C, N, and O atoms of uracil molecule can only yield three π^* and five π orbitals.⁴⁵ As for the σ^* resonances, our calculations yield three σ^* resonance energies below 5 eV. Previous studies by Burrow et al. identified the σ^* resonances at 2.26, 3.67, and 3.87 eV, which were close to our calculated positions.⁸ Furthermore, the patterns of σ_1^* and σ_2^* wave functions reported by them (Figure 2 of ref 8) also coincided with ours. Winstead and McKoy identified two σ^* resonance energies below 5 eV and two σ^* resonance energies in the 5–10 eV region, but they indicated that the peaks at 4.5 and 6 eV were likely spurious.^{13a} Leble et al. identified two σ^* resonance energies below 5 eV and one σ^* resonance at 6.7 eV.¹⁶ Dora et al. identified three σ^* resonances of Feshbach type at 6.17, 7.62, and 8.12 eV.¹⁴ Gianturco and Lucchese identified two σ^* resonances at 0.012 and 10.4 eV.¹¹ Tonzani and Greene did not report σ^* resonances.¹² Our σ_4^* , σ_5^* , and σ_6^* resonances are in the range of 5–8 eV. They might be associated with the two σ^* resonances (6 and 8.5 eV) as predicted by Winstead and McKoy.^{13a} As for the resonance widths, our calculations indicate the resonance

widths are 0.04–0.10, 0.10–0.24, and 0.20–0.42 eV for $6a''$, $7a''$, and $8a''$ π^* orbitals. As shown in Table 3, our values give π^* resonance widths in good agreement with those of previous studies by Winstead and McKoy, and Dora et al., while others gave broader widths.^{11–16} As to the σ^* resonance widths, previous studies were either incomplete or lacking. In this report, the resonance widths are found to be 1.44–1.94, 0.70–0.96, 0.45–0.88, 0.19–0.39, 0.22–0.44, and 0.18–0.42 eV for $25a'$, $26a'$, $27a'$, $28a'$, $29a'$, and $30a'$ σ^* orbitals, respectively. These values may be helpful for reference purposes in the future.

According to our stabilization calculations for the assignments of the shape resonance observed in ET spectrum on uracil, the 0.22 eV feature is ascribed to electron capture into the empty $6a''$ orbital. The 1.58 eV feature is ascribed to electron capture into the empty $7a''$ orbital. The electron addition to $25a'$ orbital may not be observed in the ET spectrum due to its short lifetime (~ 0.3 – 0.5 fs). The broad resonances at 3.83 eV can be associated with the capture into $8a''$ and $26a'$ – $27a'$ orbitals. To sum up, our stabilization calculations can provide support for the assignments of the features observed in the electron transmission spectra of the uracil.^{7,8}

4. CONCLUSION

The energies of unfilled orbitals in uracil have been studied by using the modern DFT methods. The present investigation has demonstrated that the adoption of stabilization method can allow us to distinguish the virtual orbitals from either the resonance or ODC solutions. The obtained results have demonstrated that the stabilization method in conjunction with the analytic continuation procedure via AC density functionals can yield energies and widths of temporary anion states in agreement with the experimental data and previous scattering calculations. In addition, our calculations have indicated the presence of several σ^* temporary anion states on uracil. They can certainly provide more information on the resonance states.

■ AUTHOR INFORMATION

Corresponding Author

*E-mail: hycheng@thu.edu.tw. Tel.: 011-886-4-23590248-102. Fax: 011-886-4-23590426.

■ ACKNOWLEDGMENT

We would like to thank the reviewers for valuable comments during the revision process and National Center for High-Performance Computing for the computational resources provided. This work was supported by National Science Council of Republic of China under Grant No. NSC 99-2113-M029-003.

■ REFERENCES

- (1) (a) Boudaiffa, B.; Cloutier, P.; Hunting, D.; Huels, M. A.; Sanche, L. *Science* **2000**, *287*, 1658. (b) Li, X.; Sevilla, M. D.; Sanche, L. *J. Am. Chem. Soc.* **2003**, *125*, 13668. (c) Zheng, Y.; Cloutier, P.; Hunting, D. J.; Wagner, J. R.; Sanche, L. *J. Am. Chem. Soc.* **2004**, *126*, 1002. (d) Li, X.; Sevilla, M.; Sanche, L. *J. Am. Chem. Soc.* **2003**, *125*, 13668–13669. (e) Martin, F.; Burrow, P. D.; Cai, Z.; Cloutier, P.; Hunting, D.; Sanche, L. *Phys. Rev. Lett.* **2004**, *93*, 068101. (f) Sanche, L. *Eur. Phys. J. D* **2005**, *35*, 367. (g) Sanche, L. *Mass Spectrom. Rev.* **2002**, *21*, 349.
- (2) (a) Gu, J.; Xie, Y.; Schaefer, H. F., III *J. Am. Chem. Soc.* **2005**, *127*, 1053. (b) Gu, J.; Xie, Y.; Schaefer, H. F., III *J. Am. Chem. Soc.* **2006**, *128*, 1250. (c) Sommerfeld, T. *J. Phys. Chem. A* **2004**, *108*, 9150.
- (3) (a) Berdys, J.; Anusiewicz, I.; Skurski, P.; Simons, J. *J. Am. Chem. Soc.* **2004**, *126*, 6441. (b) Simons, J. *Acc. Chem. Res.* **2006**, *39*, 772 and refs therein..
- (4) (a) Abouaf, R.; Pommier, J.; Dunet, H. *Int. J. Mass Spectrom.* **2003**, *226*, 397. (b) Denifl, S.; Ptasińska, S.; Cingel, M.; Matejcik, S.; Scheier, P.; Märk, T. D. *Chem. Phys. Lett.* **2003**, *377*, 74. (c) Hanel, G.; Gstir, B.; Denifl, S.; Scheier, P.; Probst, M.; Farizon, B.; Farizon, M.; Illenberger, E.; Märk, T. D. *Phys. Rev. Lett.* **2003**, *90*, 188104. (d) Abouaf, R.; Pommier, J.; Dunet, H. *Chem. Phys. Lett.* **2003**, *381*, 486. (e) Ptasińska, S.; Denifl, S.; Scheier, P.; Märk, T. D. *J. Chem. Phys.* **2004**, *120*, 8505. (f) Feil, S.; Gluch, K.; Matt-Leubner, S.; Scheier, P.; Limtrakul, J.; Probst, M.; Deutsch, H.; Becker, K.; Stamatovic, A.; Märk, T. D. *J. Phys. B* **2004**, *37*, 3013. (g) Abouaf, R.; Pommier, J.; Dunet, H.; Quan, P.; Nam, P.-C.; Nguyen, M. T. *J. Chem. Phys.* **2004**, *121*, 11668. (h) Denifl, S.; Candori, P.; Ptasińska, S.; Limaõ-Vieira, P.; Grill, V.; Märk, T. D.; Scheier, P. *Eur. Phys. J. D* **2005**, *35*, 391. (i) Bald, I.; Kopyra, J.; Illenberger, E. *Angew. Chem., Int. Ed.* **2006**, *45*, 4851. (j) Ptasińska, S.; Denifl, S.; Gohlke, S.; Scheier, P.; Illenberger, E.; Märk, T. D. *Angew. Chem., Int. Ed.* **2006**, *45*, 1893.
- (5) (a) Kumar, A.; Sevilla, M. D. *J. Phys. Chem. B* **2007**, *111*, 5464. (c) Kumar, A.; Sevilla, M. D. *J. Am. Chem. Soc.* **2008**, *130*, 2130.
- (6) (a) Aflatoonni, K.; Scheer, A. M.; Burrow, P. D. *Chem. Phys. Lett.* **2005**, *408*, 426. (b) Scheer, A. M.; Silvernail, C. J.; Belot, A.; Aflatoonni, K.; Gallup, G. A.; Burrow, P. D. *Chem. Phys. Lett.* **2005**, *411*, 46. (c) Aflatoonni, K.; Scheer, A. M.; Burrow, P. D. *J. Chem. Phys.* **2006**, *125*, 054301. (d) Gallup, G. A.; Fabrikant, I. I. *Phys. Rev. A* **2011**, *83*, 12706.
- (7) Aflatoonni, K.; Gallup, G. A.; Burrow, P. D. *J. Phys. Chem. A* **1998**, *102*, 6205.
- (8) Burrow, P. D.; Gallup, G. A.; Scheer, A. M.; Denifl, S.; Patsinska, S.; Maerk, T. D.; Scheier, P. *J. Chem. Phys.* **2006**, *124*, 124310.
- (9) Scheer, A. M.; Aflatoonni, K.; Gallup, G. A.; Burrow, P. D. *Phys. Rev. Lett.* **2004**, *92*, 068102-1.
- (10) Burrow, P. D. *J. Chem. Phys.* **2005**, *122*, 087105.
- (11) Gianturco, F. A.; Lucchese, R. R. *J. Chem. Phys.* **2004**, *120*, 7446.
- (12) Tonzani, S.; Greene, C. H. *J. Chem. Phys.* **2006**, *124*, 054312.
- (13) (a) Winstead, C.; McKoy, V. J. *J. Chem. Phys.* **2006**, *125*, 174304. (b) Winstead, C.; McKoy, V. J. *J. Chem. Phys.* **2006**, *125*, 244302. (c) Winstead, C.; McKoy, V.; Sanchez, S. d'A. *J. Chem. Phys.* **2007**, *127*, 85105.
- (14) Dora, A.; Tennyson, J.; Bryjko, L.; van Mourik, T. *J. Chem. Phys.* **2009**, *130*, 164307.
- (15) Gianturco, F. A.; Sebastianelli, F.; Lucchese, R. R.; Baccarelli, I.; Sanna, N. *J. Chem. Phys.* **2008**, *128*, 174302.
- (16) Yalunin, S.; Leble, S. B. *Eur. Phys. J. Spec. Top.* **2007**, *144*, 115.
- (17) Sanche, L.; Schulz, G. *J. Phys. Rev. A* **1972**, *5*, 1672.
- (18) Jordan, K. D.; Burrow, P. D. *Chem. Rev.* **1987**, *87*, 557.
- (19) Koopmans, T. *Physica* **1934**, *1*, 104.
- (20) Kohn, W.; Sham, L. *J. Phys. Rev. A* **1965**, *140*, 1133.
- (21) Simons, J. *J. Phys. Chem. A* **2008**, *112*, 6401.
- (22) Rienstra-Kiracofe, J. C.; Tschumper, G. S.; Schaefer, H. F., III; Nandi, S.; Ellison, G. B. *Chem. Rev.* **2002**, *102*, 231.
- (23) Chai, J.-D.; Head-Gordon, M. *Phys. Chem. Chem. Phys.* **2008**, *10*, 6615.
- (24) Vydrov, O. A.; Scuseria, G. E.; Perdew, J. P. *J. Chem. Phys.* **2007**, *126*, 154109.
- (25) Yanai, T.; Tew, D. P.; Handy, N. C. *Chem. Phys. Lett.* **2004**, *393*, 51.
- (26) (a) Iikura, H.; Tsuneda, T.; Yanai, T.; Hirao, K. *J. Chem. Phys.* **2001**, *115*, 3540. (b) Tsuneda, T.; Song, J.-W.; Suzuki, S.; Hirao, K. *J. Chem. Phys.* **2010**, *174*101.
- (27) (a) Tozer, D. J.; De Proft, F. *J. Phys. Chem. A* **2005**, *109*, 8923. (b) Tozer, D. J.; De Proft, F. *J. Chem. Phys.* **2007**, *127*, 034108. (c) De Proft, F.; Sablon, N.; Tozer, D. J.; Geerlings, P. *Faraday Discuss.* **2007**, *135*, 151. (d) Sablon, N.; De Proft, F.; Geerlings, P.; Tozer, D. J. *Phys. Chem. Chem. Phys.* **2007**, *9*, 5880. (e) Teale, A. M.; De Proft, F.; Tozer, D. J. *J. Chem. Phys.* **2008**, *129*, 044110. (f) Hajagató, B.; Deleuze, M. S.; Tozer, D. J.; De Proft, F. *J. Chem. Phys.* **2008**, *129*, 084308. (g) Peach, M. J. G.; De Proft, F.; Tozer, D. J. *J. Phys. Chem. Lett.* **2010**, *1*, 2826.

- (28) (a) Falcetta, M. F.; Jordan, K. D. *J. Phys. Chem.* **1990**, *94*, 5666.
 (b) Falcetta, M. F.; Jordan, K. D. *J. Am. Chem. Soc.* **1991**, *113*, 2903.
 (c) Falcetta, M. F.; Jordan, K. D. *Chem. Phys. Lett.* **1999**, *300*, 588.
 (d) Falcetta, M. F.; Choi, Y.; Jordan, K. D. *J. Phys. Chem. A* **2000**, *104*, 9605.
- (29) Burrow, P. D.; Howard, A. E.; Johnston, A. R.; Jordan, K. D. *J. Phys. Chem.* **1992**, *96*, 7570.
- (30) (a) Juang, C.-Y.; Chao, J. S.-Y. *J. Phys. Chem.* **1994**, *98*, 13506.
 (b) Chen, C.-S.; Feng, T.-H.; Chao, J. S.-Y. *J. Phys. Chem.* **1995**, *99*, 8629.
 (c) Wei, Y.-H.; Cheng, H.-Y. *J. Phys. Chem. A* **1998**, *102*, 3560.
- (31) (a) Hazi, A. U.; Taylor, H. S. *Phys. Rev. A* **1970**, *1*, 1109.
 (b) Taylor, H. S. *Adv. Chem. Phys.* **1970**, *18*, 91. (c) Fels, M. F.; Hazi, A. U. *Phys. Rev. A* **1972**, *5*, 1236. (d) Taylor, H. S.; Hazi, A. U. *Phys. Rev. A* **1976**, *14*, 2071.
- (32) (a) Cheng, H.-Y.; Shih, C.-C. *J. Phys. Chem. A* **2009**, *113*, 1548.
 (b) Cheng, H.-Y.; Shih, C.-C.; Chang, J.-T. *J. Phys. Chem. A* **2009**, *113*, 9551. (c) Cheng, H.-Y.; Chang, J.-T.; Shih, C.-C. *J. Phys. Chem. A* **2010**, *113*, 2920. (d) Cheng, H.-Y.; Chen, C.-W.; Chang, J.-T.; Shih, C.-C. *J. Phys. Chem. A* **2011**, *115*, 84.
- (33) (a) Dunning, T. H., Jr. *J. Chem. Phys.* **1970**, *53*, 2823.
 (b) Dunning Jr., T. H.; Hay, P. J. In *Methods of Electronic Structure Theory*; Schaefer, H. F., III, Ed.; Plenum Press: New York, 1977; Vol. 2.
- (34) (a) Dunning, T. H., Jr. *J. Chem. Phys.* **1989**, *90*, 1007.
 (b) Kendall, R. A.; Dunning, T. H., Jr.; Harrison, R. J. *J. Chem. Phys.* **1992**, *96*, 6769.
- (35) (a) The midpoint method is applicable when compared its results with those obtained from the more rigorous analytic continuation method (ref 19 in ref 30a). (b) In cases where the stabilized temporary anion resonance of interest is well separated from ODC levels over the range of α values examined, the energy of the resonance state can be estimated simply from inspection of the stabilization graph (ref 28d).
- (36) (a) Jordan, K. D. *Chem. Phys.* **1975**, *9*, 199. (b) Chao, J. S.-Y.; Falcetta, M. F.; Jordan, K. D. *J. Chem. Phys.* **1990**, *93*, 1125. (c) Chao, J. S.-Y. *Chem. Phys. Lett.* **1991**, *179*, 169. (d) Yu, L.; Chao, J. S.-Y. *J. Chin. Chem. Soc.* **1993**, *40*, 12.
- (37) (a) Frey, R. F.; Simons, J. *J. Chem. Phys.* **1986**, *84*, 4462.
 (b) Thompson, T. C.; Truhlar, D. G. *Chem. Phys. Lett.* **1982**, *92*, 71. (c) The resonance energies and widths can also be obtained by means of density-of-state method Mandelsham, V. A.; Ravuri, T. R.; Taylor, H. S. *Phys. Rev. Lett.* **1993**, *70*, 1932. (d) Simons's formula Simons, J. *J. Chem. Phys.* **1981**, *75*, 2465. (e) and Löwdin's scheme Löwdin, P.-O. *Int. J. Quantum Chem.* **1985**, *27*, 495.
- (38) Zhao, Y.; Truhlar, D. G. *J. Chem. Phys.* **2006**, *125*, 194101.
- (39) Perdew, J. P.; Burke, K.; Ernzerhof, M. *Phys. Rev. Lett.* **1996**, *77*, 3865.
- (40) Zhao, Y.; Truhlar, D. G. *Theor. Chem. Acc.* **2008**, *120*, 215.
- (41) Zhao, Y.; Truhlar, D. G. *J. Phys. Chem. A* **2006**, *110*, 13126.
- (42) (a) Grimme, S. *J. Chem. Phys.* **2006**, *124*, 034108. (b) Schwabe, T.; Grimme, S. *Phys. Chem. Chem. Phys.* **2006**, *8*, 4398. (c) Schwabe, T.; Grimme, S. *Phys. Chem. Chem. Phys.* **2007**, *9*, 3397.
- (43) Frisch, M. J.; Trucks, G. W.; Schlegel, H. B.; Scuseria, G. E.; Robb, M. A.; Cheeseman, J. R.; Scalmani, G.; Barone, V.; Mennucci, B.; Petersson, G. A.; Nakatsuji, H.; Caricato, M.; Li, X.; Hratchian, H. P.; Izmaylov, A. F.; Bloino, J.; Zheng, G.; Sonnenberg, J. L.; Hada, M.; Ehara, M.; Toyota, K.; Fukuda, R.; Hasegawa, J.; Ishida, M.; Nakajima, T.; Honda, Y.; Kitao, O.; Nakai, H.; Vreven, T.; Montgomery, Jr., J. A.; Peralta, J. E.; Ogliaro, F.; Bearpark, M.; Heyd, J. J.; Brothers, E.; Kudin, K. N.; Staroverov, V. N.; Kobayashi, R.; Normand, J.; Raghavachari, K.; Rendell, A.; Burant, J. C.; Iyengar, S. S.; Tomasi, J.; Cossi, M.; Rega, N.; Millam, J. M.; Klene, M.; Knox, J. E.; Cross, J. B.; Bakken, V.; Adamo, C.; Jaramillo, J.; Gomperts, R.; Stratmann, R. E.; Yazyev, O.; Austin, A. J.; Cammi, R.; Pomelli, C.; Ochterski, J. W.; Martin, R. L.; Morokuma, K.; Zakrzewski, V. G.; Voth, G. A.; Salvador, P.; Dannenberg, J. J.; Dapprich, S.; Daniels, A. D.; Farkas, O.; Foresman, J. B.; Ortiz, J. V.; Cioslowski, J.; Fox, D. J. *Gaussian 09*, Revision A.02; Gaussian, Inc.: Wallingford, CT, 2009.
- (44) (a) Vydrov, O. A.; Scuseria, G. E. *J. Chem. Phys.* **2005**, *122*, 184107. (b) Dutoi, A. D.; Head-Cordan, M. *Chem. Phys. Lett.* **2006**, *422*, 230.
- (45) Winstead, C.; McKoy, V. *J. Chem. Phys.* **2008**, *129*, 77101.
- (46) Compton, R. N.; Yoshioka, Y.; Jordan, K. D. *Theor. Chim. Acta* **1980**, *54*, 259.